

See discussions, stats, and author profiles for this publication at: <https://www.researchgate.net/publication/259723376>

# The Role of Enthalpy – Entropy Compensation Interactions in Determining the Conformational Propensities of Amino Acid Residues in Unfolded Peptides.

ARTICLE *in* THE JOURNAL OF PHYSICAL CHEMISTRY B · JANUARY 2014

Impact Factor: 3.3 · DOI: 10.1021/jp500181d · Source: PubMed

---

CITATIONS

12

---

READS

34

3 AUTHORS, INCLUDING:



Reinhard Schweitzer-Stenner

Drexel University

219 PUBLICATIONS 4,372 CITATIONS

SEE PROFILE

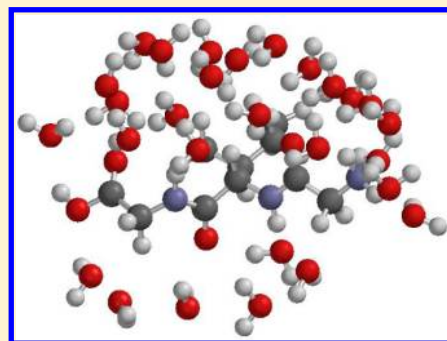
# Role of Enthalpy–Entropy Compensation Interactions in Determining the Conformational Propensities of Amino Acid Residues in Unfolded Peptides.

Siobhan E. Toal,<sup>†</sup> Daniel J. Verbaro,<sup>†,‡,§</sup> and Reinhard Schweitzer-Stenner<sup>\*,†</sup>

<sup>†</sup>Departments of Chemistry and <sup>‡</sup>Biology, Drexel University, 3141 Chestnut Street, Philadelphia, Pennsylvania 19104, United States

**S** Supporting Information

**ABSTRACT:** The driving forces governing the unique and restricted conformational preferences of amino acid residues in the unfolded state are still not well understood. In this study, we experimentally determine the individual thermodynamic components underlying intrinsic conformational propensities of these residues. Thermodynamic analysis of ultraviolet-circular dichroism (UV-CD) and <sup>1</sup>H NMR data for a series of glycine capped amino acid residues (i.e., G-x-G peptides) reveals the existence of a nearly exact enthalpy–entropy compensation for the polyproline II– $\beta$  strand equilibrium for all investigated residues. The respective  $\Delta H_{\beta}$ ,  $\Delta S_{\beta}$  values exhibit a nearly perfect linear relationship with an apparent compensation temperature of  $295 \pm 2$  K. Moreover, we identified iso-equilibrium points for two subsets of residues at 297 and 305 K. Thus, our data suggest that within this temperature regime, which is only slightly below physiological temperatures, the conformational ensembles of amino acid residues in the unfolded state differ solely with respect to their capability to adopt turn-like conformations. Such iso-equilibria are rarely observed, and their existence herein indicates a common physical origin behind conformational preferences, which we are able to assign to side-chain dependent backbone solvation. Conformational effects such as differences between the number of sterically allowed side chain rotamers can contribute to enthalpy and entropy but not to the Gibbs energy associated with conformational preferences. Interestingly, we found that alanine, aspartic acid, and threonine are the only residues which do not share these iso-equilibria. The enthalpy–entropy compensation discovered as well as the iso-equilibrium and thermodynamics obtained for each amino acid residue provide a new and informative way of identifying the determinants of amino acid propensities in unfolded and disordered states.



## INTRODUCTION

The classic paradigms governing protein folding and bio-structure–function relationships have undergone vast overhauls in the scientific community. This is primarily due to the discovery of intrinsically disordered proteins (IDPs), which lack a well-defined structure under physiological conditions yet participate in complex biological functions.<sup>1–5</sup> The disorder in IDPs has been described as random coil-like. Therefore, IDPs are generally considered as structurally similar to unfolded proteins. For a long period of time, however, the unfolded state has been neglected, in part due to insufficient methods to study it but also due to the long-standing assumption that it can be described as an optimal solvated random coil with conformational distributions governed nearly exclusively by steric backbone–backbone interactions.<sup>6–9</sup> If this model was indeed valid it would be sufficient to treat the unfolded state as an amorphous homopolymeric entity of high entropy, and its structure and size would be independent of amino acid composition.<sup>10,11</sup> However, multiple lines of evidence have since emerged suggesting that this picture is way too simplistic. First, numerous NMR studies revealed residual structure in IDPs (and unfolded proteins) caused by nonlocal hydrophobic and intraprotein hydrogen bonding interactions.<sup>12–17</sup> Second, amino acids residues do not sample the entire sterically allowed

Ramachandran space. Instead they display very distinct conformational preferences in short peptides,<sup>18–22</sup> which define the initial conditions for the formation of residual structure in longer unfolded peptides and proteins. This is illustrated by Figure 1, which shows an earlier obtained Ramachandran plot for the alanine residue of cationic GAG.<sup>21</sup> A practically identical plot was observed for the classical model system, the alanine

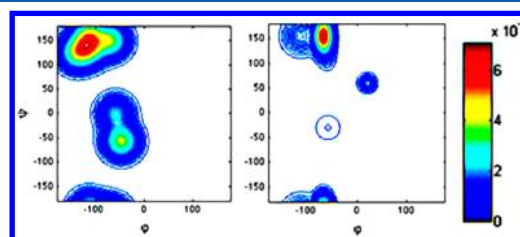


**Figure 1.** (left) Ramachandran plot of a random coil-like distribution of conformational ensembles; (right) Ramachandran plot of the alanine dipeptide in water as reported by Toal et al.<sup>22</sup>

**Received:** January 7, 2014

**Revised:** January 14, 2014

**Published:** January 14, 2014

dipeptide.<sup>22</sup> Apparently, alanine predominantly samples the polyProline II (pPII) conformation, which is a rather restricted subspace of the sterically allowed Ramachandran plot depicted in Figure 1b. Contrary to the single broad distribution that the classical Ramachandran plot in Figure 1 displays, distribution functions obtained for the amino acid residues are often bimodal in the upper left quadrant and allow one to discriminate between subdistributions of pPII and  $\beta$ -strand like conformations. Generally, the combined conformational space of pPII and the  $\beta$ -strand was found to be much more restricted than a typical random coil distribution in the upper left quadrant in the Ramachandran plot.<sup>18,21</sup> In addition to these conformational restrictions, a subset of the amino acid residues exhibit unusually high propensities for conformations found in turns, which we term “turn-like” in the following.<sup>10,11,19</sup> In general, conformational ensembles for amino acid residues are varied, unique, and unexplainable in the context of pure steric interactions.

The physical origin behind this restricted conformational sampling of the Ramachandran space by practically all amino acid residues in general and of their different conformational distributions in particular remains largely unclear. Most theories, however, and a limited number of experiments emphasize the role of water solvation for the stabilization of pPII,<sup>10,11,23–25</sup> while they still disagree on the underlying mechanism. They suggest a variety of causes encompassing direct hydrogen bond bridge formation,<sup>23</sup> electrostatic and steric effects,<sup>26,27</sup> and optimal water packing in the hydration shell.<sup>24</sup>

Many of the attempts to elucidate the conformational biases of amino acid residues generally focus on Gibbs free energy differences between populated conformations.<sup>27–30</sup> However, the reliability of any thermodynamic model should be checked with regard to its capability to rationalize concomitant changes in enthalpy (internal energy) and entropy. For instance, it is well documented that pPII conformations are stabilized enthalpically, while more extended  $\beta$ -strands are entropically favored.<sup>22,31–34</sup> This indicates at least a partial enthalpy–entropy compensation for the equilibrium between these conformers. Early theories on structural transitions of biomolecules suggest that direct and indirect solute–solvent (water) interactions could bring about a nearly exact thermodynamic compensation of very large enthalpic and entropic changes associated with conformational transitions of biomolecules (i.e., between pPII and  $\beta$  in the case of amino acid residues), thus yielding very low Gibbs energies.<sup>35–38</sup> Hence, all the important thermodynamic information which should provide physical insight into why certain conformational propensities are stabilized becomes lost within minor  $\Delta G$  changes.

This study is aimed at elucidating the individual thermodynamic contributions underlying conformational propensities in order to shed light on the factors driving local order. If a common thermodynamic cause for the different propensities of amino acid residues exists, enthalpy and entropy will be nearly perfectly linearly related, thus reflecting a very narrow distribution of compensation temperatures at which a substantial part of the total Gibbs energy disappears due to enthalpy–entropy cancelation.<sup>38</sup> In order to check whether this scenario applies to individual amino acid residues in unfolded peptides, we determined the enthalpic and entropic contributions to the Gibbs energy landscape of GxG model peptides in aqueous solution by a global analysis of their temperature

dependent ultraviolet-circular dichroism (UV-CD) and <sup>1</sup>H NMR spectra. This analysis was based on sets of experimentally determined conformational distributions, which we recently obtained for these peptides at room temperature.<sup>18–20,39</sup> We herein identify a common nearly exact enthalpic–entropic compensation effect,<sup>40</sup> which for a majority of amino acid residues in aqueous solution causes an iso-equilibrium at near physiological temperatures. This is a rarely observed phenomenon which shows that these amino acid residues share a common compensation temperature at which the solvation Gibbs energy is zero.<sup>38</sup> Only three amino acid residues, A, D, and T, deviate from this picture, most likely due to additional intrapeptide interactions. We propose the average compensation temperature of the investigated set of peptides as a measure of the goodness of the solvent which determines its capability to stabilize a statistical coil over partially or completely folded states of proteins.

## MATERIALS AND METHODS

**Materials.** All L-Glycyl-X-Glycine (GxG, X = alanine, lysine, leucine, isoleucine, arginine, phenylalanine, methionine, serine, valine, aspartic acid, glutamic acid, threonine) peptides were purchased from Genscript Corp. with >98% purity and purified via dialysis in an aqueous HCl medium and subsequent lyophilization. For <sup>1</sup>H NMR measurements, each peptide was dissolved in a solution of 90% H<sub>2</sub>O/10% D<sub>2</sub>O (1% TMS) at a concentration of 0.1 M. For CD measurements, each peptide was dissolved in a solution of H<sub>2</sub>O at a concentration of 0.01 M. The pH was adjusted to 2 with HCl for all experiments.

**NMR Spectroscopy.** Amide proton <sup>3</sup>J(H<sup>N</sup>H <sup>$\alpha$</sup> ) coupling constants for all peptides were determined using <sup>1</sup>H NMR. The spectra were recorded on a Varian 500 MHz FT-NMR with a 5 mm HCN triple resonance probe. Temperature was controlled using a Varian VT controller, and spectra were collected between 25 and 60 °C in increments of 5 °C. Each sample was allowed to equilibrate at every temperature for 2 min before an experiment was started. For GIG and GVG, the amide proton signals became unresolvable above 40 °C due to signal overlap. Hence, data above this temperature were not used in the analysis. Collection and analysis of <sup>1</sup>H NMR spectra as well as determination of <sup>3</sup>J(H<sup>N</sup>H <sup>$\alpha$</sup> ) constants as a function of temperature were conducted as described in previous studies.<sup>22,32</sup>

**Ultraviolet Circular Dichroism.** UV-CD spectra were measured on a Jasco J-810 spectropolarimeter (Jasco, Inc.) purged with N<sub>2</sub>. The 0.01 M sample was loaded into a 50  $\mu$ m International Crystals Laboratories (ICL) cell. Spectra were measured between 180 nm and 300 nm with a 500 nm/min scan speed, a 1 s response time, a 0.05 data pitch, and a 5 nm bandwidth. Spectra were taken from 10 to 85 °C with 5 °C increments using a Peltier controller (model PTC-423S). All spectra were corrected using appropriate background subtraction. UVCD spectra for the aromatic residues were not obtained.

## RESULTS

**Thermodynamics of Conformational Preferences.** We recently reported detailed conformational analyses of GxG model peptides in water based on a global analysis of amide I' bands of IR, Raman, and vibrational circular dichroism spectra as well as of 2D NMR *J* coupling parameters.<sup>18–21</sup> The advantage of such an approach is the ability to derive residue-

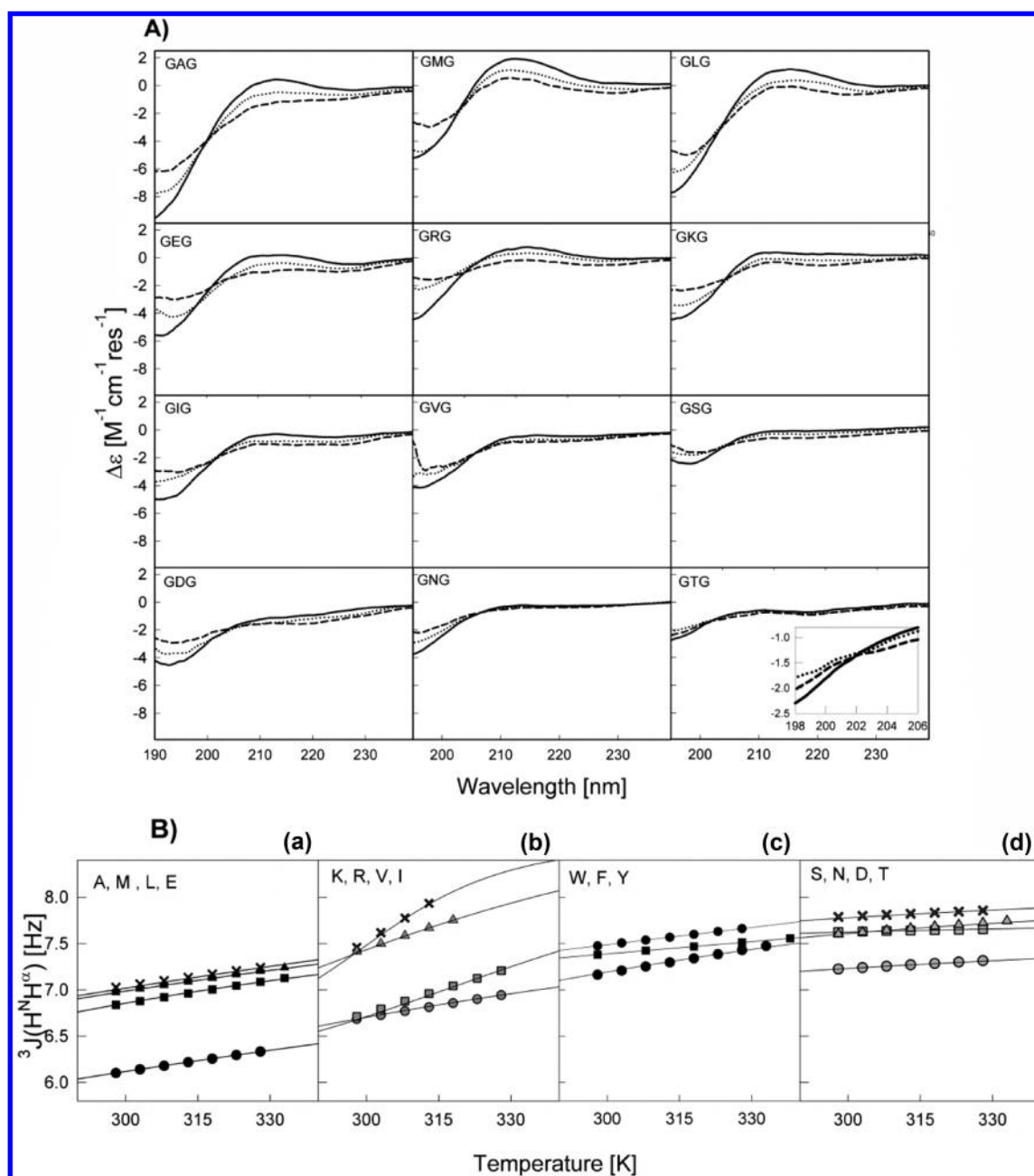


**Figure 2.** (A) UV-CD spectra as a function of temperature for GAG, GKG, GVG, and GDG. For clarity, only spectra taken at 10 °C (solid line), 50 °C (dotted line), and 90 °C (dashed line) are shown. (B)  $^3J(\text{H}^N, \text{H}^\alpha)$  [Hz] coupling constants as a function of temperature for all amino acid residues. The solid lines result from the thermodynamic model described in the text. Panel a displays alanine (circles), methionine (squares), leucine (triangles), glutamic acid (crosses). Panel b displays lysine (circles), arginine (squares), valine (triangles), isoleucine (crosses). Panel c displays tryptophan (circles), phenylalanine (squares), tyrosine (triangles). Panel d displays serine (circles), asparagine (squares), valine (triangles), isoleucine (crosses).

level conformational information from each spectroscopic technique and combine them with statistical models that describe the entire conformational manifold of the peptides' guest residues. The obtained results allow us to subdivide the amino acid residues investigated here into categories according to their pPII propensity. Alanine was found to stand out with an exceptionally high pPII propensity of 0.72.<sup>21,22</sup> Category number 2 contains residues like L and K with a modest dominance of pPII over a substantial  $\beta$ -strand fraction.<sup>18,21</sup> The third category contains branched aliphatic and aromatic groups (V, I, F), which display comparatively higher  $\beta$  strand and turn propensities.<sup>21</sup> The fourth category of peptides contains

residues with short polar and/or ionizable central residues (D, T, N, C) and a higher than average content of turn-like conformations.<sup>19,20</sup>

To characterize these conformational ensembles in thermodynamic terms, we herein analyze the temperature dependence of the UV-CD and  $^1\text{H}$  NMR spectra of GxG peptides by using a method similar to those of Toal et al.<sup>22,32</sup> and Cho et al.<sup>41–43</sup> These authors assumed that conformational redistributions for short alanine based peptides can be described by simple two-state pPII- $\beta$  models. The thermodynamic analyses of non-alanine GxG peptides, however, are complicated by the presence of turn-like conformations, which for aspartic acid



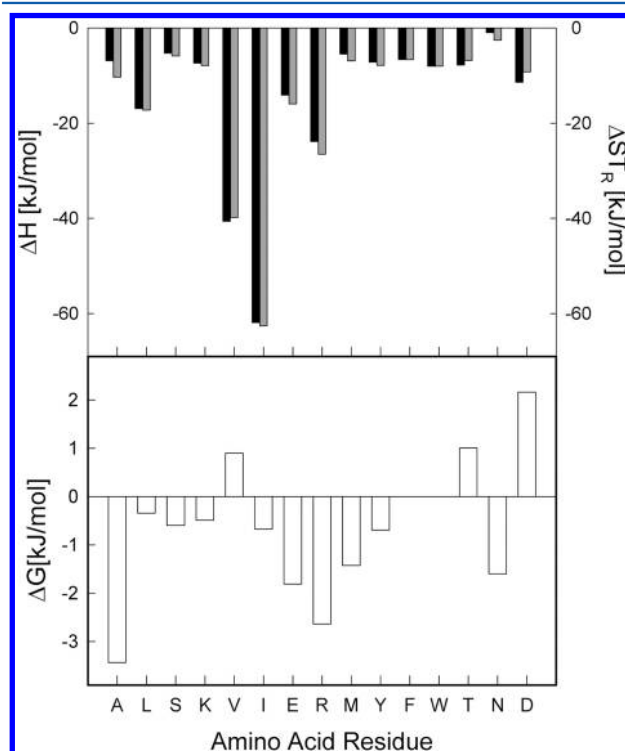
constitute 32% of the conformational ensemble. Recently, however, Rybka et al. showed that these conformations are generally thermostable.<sup>20</sup> If this notion applies to all residues investigated, a quasi two-state thermodynamic model with temperature independent fractions of turn conformations is a suitable approximation for this study. To check the validity of such a quasi two-state model analysis, we first measured the far UV-CD spectra as a function of temperature for all investigated GxG peptides. These spectra are exhibited in Figure 2. At low temperatures, spectra of all peptides display a negatively biased couplet with the negative maximum at approximately 195 nm, which is diagnostic of a substantial sampling of pPII conformations.<sup>44–46</sup> With increasing temperature, the dichroism at 215 nm ( $\Delta\epsilon_{215}$ ) and the negative maximum ( $\Delta\epsilon_{195}$ ) decrease, indicating a conformational redistribution toward more  $\beta$ -strand-like conformations.<sup>31,43,47</sup> The pPII content as indicated by  $\Delta\epsilon_{195}$  and  $\Delta\epsilon_{215}$  differs for each peptide at each temperature, confirming the notion that each amino acid residue has distinct conformational preferences in the unfolded state. The pPII preference as indicated by the UVCD spectra for each residue at temperatures lower than or equal to room temperature qualitatively agrees with those explicitly derived by Hagarman et al.,<sup>6,7,10</sup> i.e., the pPII preference decreases in the following order: A, M > L, E, R, K >> I, V, S > D, N, T. Amino acids with high turn propensities (D, N, T, S) additionally exhibit a shallow negative maximum at approximately 220 nm.<sup>7</sup> However, the temperature dependence of this marker is modest, and indeed all CD spectra exhibit a clear isodichroic point ( $\approx 204$  nm) confirming that the conformational ensemble at all investigated temperatures is dominated by two states (pPII and  $\beta$ ) and a quasi two-state model considering only exchanges between pPII and  $\beta$ -strand is a suitable approach.

To gain site-specific information, the  $^3J(\text{H}^{\text{N}}\text{H}^{\alpha})$  coupling constants were measured as a function of temperature. These constants reflect the average  $\Phi$  value of the central x-residue according to the Karplus relationship<sup>48,49</sup> and are thus useful observables for assessing residue-level conformational populations. In line with the above-mentioned results, we constructed a simple thermodynamic model that considers (1) redistributions among extended structures (pPII- $\beta$ ) as temperature dependent and (2) temperature independent turn populations. Hence, the temperature dependence of corresponding  $^3J$  values can be written as<sup>9</sup>

$$^3J(T) = \frac{^3J_{\text{pPII}} + ^3J_{\beta} \exp\left[-\left(\frac{\Delta H_{\beta}}{RT} - \frac{\Delta H_{\beta} - \Delta G_{\beta}(T_{\text{R}})}{RT_{\text{R}}}\right)\right]}{1 + \exp\left[-\left(\frac{\Delta H_{\beta}}{RT} - \frac{\Delta H_{\beta} - \Delta G_{\beta}(T_{\text{R}})}{RT_{\text{R}}}\right)\right]} \times (\chi_{\text{pPII}} + \chi_{\beta}) + \sum_i J_{\text{T},i} \chi_{\text{T},i} \quad (1)$$

where  $^3J_i$  and  $\chi_i$  are the  $J$ -coupling constants and normalized mole fractions of each peptide's unique conformations:  $i = \text{pPII}, \beta, \text{turn}$ .  $\Delta G(T_{\text{R}})$  is the corresponding Gibbs free energy difference between pPII and  $\beta$  at room temperature  $T_{\text{R}}$ . The values for  $\Delta G(T_{\text{R}})$  were calculated from earlier reported pPII/ $\beta$  mole fraction ratios.<sup>9,10</sup> Reference  $^3J_{\text{F}}$ -values were calculated as averages over the unique  $\phi, \psi$  subdistributions of the  $i$ th conformation for each investigated residue using the Karplus equation.<sup>20</sup> Thus, only  $\Delta H_{\beta}$  was used as a free parameter in the fit of eq 1 to experimental  $^3J(\text{H}^{\text{N}}\text{H}^{\alpha})(T)$ . We obtained very good fits to the experimental data using this rather restrictive approach (Figure 2B). The exception to this is valine, for which

we had to assume a temperature dependence of its unusually large (11%)  $\gamma$ -turn population (eq S1 in the Supporting Information). The thermodynamic values  $\Delta H$  and  $\Delta S$  obtained from our fits and the corresponding room temperature  $\Delta G$  values are visualized in Figure 3 and listed for reference in



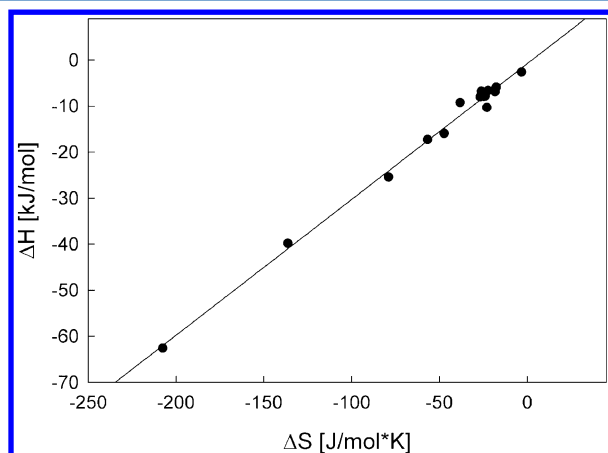
**Figure 3.**  $\Delta H$  (gray bars) and  $T_{\text{R}}\Delta S$  (black bars) values (upper panel) and  $\Delta G$  (lower panel) obtained for the indicated residues (upper Panel).

Table S2 in the Supporting Information. Immediately, one can see from the wide distribution of thermodynamic values that amino acids substantially differ with regard to their enthalpic and entropic contributions to the pPII/ $\beta$  equilibrium. Generally, our data indicate that enthalpic and the entropic contributions far exceed the Gibbs energy at room temperature, which is diagnostic of a near-exact enthalpy–entropy compensation.<sup>38</sup>

**Enthalpy–Entropy Compensation.** A closer look at Figure 3 reveals that not only are the  $\Delta H$  and  $\Delta S$  values of different residues vastly dissimilar, but in addition, individual  $\Delta H/\Delta S$  values for each amino acid residue seem to compensate each other to an extent which minimizes the Gibbs free energy for all residues. A balance between entropic losses and enthalpic gains upon structure formation is ubiquitous to protein folding processes and all types of interactions involving weak, van der Waals governed forces.<sup>36</sup> However, exact enthalpy–entropy compensation (in contrast to a mere correlation) is an interesting phenomena per se and implies that  $\Delta H = T_{\text{c}}\Delta S$  and hence  $\Delta G = 0$  at  $T = T_{\text{c}}$ .  $T_{\text{c}}$  is termed the compensation temperature. With regard to the GxG peptides investigated in this study,  $T_{\text{c}}$  could then be identified with the average transition temperature for the pPII  $\rightleftharpoons$   $\beta$  equilibrium. Alternatively, only a fraction of the Gibbs energy could be subject to compensation, in this case:<sup>35</sup>

$$\Delta H = \alpha - T_{\text{c}}\Delta S \quad (2)$$

Therefore, an exact statistically significant linear fit to  $\Delta H/\Delta S$  values indicates that all investigated processes can be related to exactly the same compensation temperature  $T_c$  and Gibbs free energy, whereas statistically significant data scattering reflects a distribution of similar compensation temperatures. To determine the category of enthalpy–entropy compensation reflected by our thermodynamic data, we plotted the enthalpy and entropy differences between pPII and  $\beta$  for all amino acid residues investigated. As shown in Figure 4, we obtained a



**Figure 4.** Plot of  $\Delta H$  versus  $\Delta S$  values obtained from a thermodynamic analysis of  $^3J(\text{H}^{\text{N}}\text{H}^{\alpha})$  ( $T$ ) data of all investigated amino acid residues. The solid line results from the linear least-squares fit described in text.

nearly perfect linear relationship when fitting the data with eq 2. The fit yielded a  $T_c$ -value of  $295 \pm 2$  K and an  $\alpha$ -value of  $-0.77$  kJ/mol. The high correlation coefficient of 0.98 indicates that the compensation temperatures for the individual GxGs should be very similar. These parameter values will be considered further in the Discussion.

**Iso-Equilibrium Points.** Technically, it is difficult to establish a common compensation temperature for a set of correlating  $\Delta H$ ,  $\Delta S$  pairs owing to their statistical uncertainties, which per se rule out a perfect correlation. The high value obtained for the correlation coefficient of the fit to eq 2 in Figure 4 suggests that our data pairs might be sufficiently accurate and precise to achieve this goal. In this case, we should be able to identify a temperature at which at least a substantial number of the investigated amino acid residues exhibit nearly the same Gibbs energy difference between pPII and  $\beta$ .<sup>38</sup> In order to determine whether such an iso-equilibrium point exist for the amino acid residues, we calculated the mole fraction ratio of pPII and  $\beta$  for all peptides as a function of temperature (Figure 5). We indeed found that there are two closely spaced iso-equilibria representing two subsets of amino acid residues. The first iso-equilibrium cluster (IE1) occurs at approximately 302 K and contains the amino acid residues L, V, I, S, K, Y, W, and F; the second iso-equilibrium point (IE2) occurs at a slightly higher temperature (approximately 312 K) and contains E, R, M, N (parts a and b of Figure 5, respectively). Notably, IE1 contains mostly amino acids with short bulky side chains (L, I, V) as well as the aromatics (Y, W, F), with serine as an exception. This equilibrium point is characterized by nearly equal mole fractions of pPII and  $\beta$  ( $\chi_{\text{pPII, IE1}}/\chi_{\beta, \text{IE1}} \approx 1$ ) and hence indicates a rather iso-energetic free energy landscapes in the upper left quadrant of the Ramachandran plot at the

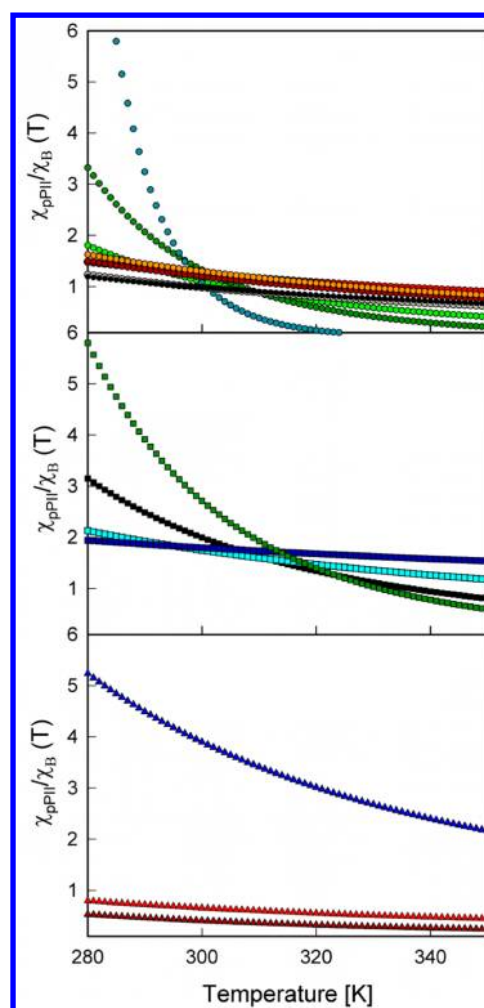


**Figure 5.** Temperature dependence of  $\chi_{\text{pPII}}/\chi_{\beta}$  for all investigated amino acid residues. (upper panel) The first iso-equilibrium cluster (IE1) containing amino acid residues I (turquoise), V (green), L (light green), Y (orange), S (red), W (gray), F (black). (middle panel) The second iso-equilibrium cluster (IE2) containing R (green), E (black), M (aqua), and N (blue) residues. (lower panel) Remaining  $\chi_{\text{pPII}}/\chi_{\beta}$  for alanine (blue), aspartic acid (dark red), and threonine (red).

corresponding temperature (302 K). IE2 is characterized by  $\chi_{\text{pPII, IE2}}/\chi_{\beta, \text{IE2}} \approx 2$ , indicating a much stronger bias for pPII for these amino acids.

In order to determine the average compensation temperature for these two subsets, we plotted the respective  $\Delta H$  and  $\Delta S$  values separately and subjected them to a linear regression. The results in Figure S1 in the Supporting Information reveal a nearly perfect linearity for both fits. The respective compensation temperatures obtained from these fits are  $T_{c1} = 297 \pm 4$  K and  $T_{c2} = 305 \pm 3$  K, the respective axis values are  $\alpha_1 = -0.3 \pm 0.3$  kJ/mol and  $\alpha_2 = 1.4 \pm 0.2$  kJ/mol. The corresponding correlation coefficients are 0.999.

When these two clusters are removed from analysis, we are left with only three amino acid residues, namely, alanine, aspartic acid, and threonine (Figure 5c). We like to emphasize again that these real compensation temperatures differ from the lower  $T_c$ -value obtained from the fit to eq 2. Only in the case of a perfect fit (correlation coefficient of 1) would this  $T_c$ -value coincide with the temperature associated with a single iso-equilibrium point.

## DISCUSSION

**Existence of Statistically Significant Enthalpy–Entropy Compensation.** The combined iso-equilibria and near-exact  $\Delta H/\Delta S$  compensation among the investigated GxG peptides implies that there is a common mechanistic effect behind conformational preference in the unfolded state. Enthalpy–entropy compensation effects have been reported in a wide array of different protein folding and binding phenomena.<sup>36,38,50</sup> However, the statistical accuracy, the existence itself of “extra-thermodynamic” enthalpy–entropy compensation effects, and the physical basis for such effects has been a matter of debate in a range of literature.<sup>38,50,51</sup> Krug et al. presented an analysis of such compensations and derived tests for distinguishing between extra-thermodynamic factors and statistical compensation.<sup>51</sup> Following their protocol, we found that the linearity of our  $\Delta H/\Delta S$  data is not a mere statistical artifact (Supporting Information). In this context, it is important to also note that the critical assessment of linear enthalpy–entropy relationships provided by Krug et al. is based on van’t Hoff and Arrhenius plots, which indeed are prone to strong statistical correlations between  $\Delta H$  and  $\Delta S$ . Recently, Liu and Gao showed that if the experimental errors along the  $\Delta H$  and  $\Delta S$  plane are significantly less than the range of the experimental values, the data are indicative of a real compensation effect.<sup>38</sup> Error analysis reveals that the largest associated errors are still significantly smaller than the range of experimentally obtained values (Figure S2 and Table S3 in the Supporting Information).

In addition, the iso-equilibria we obtained indicates that at least a large subset of investigated amino acid residues shares a common transition temperature, and hence the  $\Delta H/\Delta S$  compensation is real and justified. Although one expects, to a certain degree, that enthalpy and entropy will be opposing driving forces in conformational transitions, an exact linear compensation for similar, though not identical, thermodynamic processes (i.e., in our case the pPII/ $\beta$  equilibrium of different residues) is rarely observed. If, for instance, compensation temperatures for related processes were slightly different, the  $\Delta H$  and  $\Delta S$  values would not be exactly reproduced by the linear fit, they may still show significant correlation. The obtained  $T_c$ -value in this case would then be considered as representative of a set of slightly different underlying compensation temperatures. Therefore, one may say that the better the correlation obtained, the more similar are the respective compensation temperatures and the more likely it is that a common mechanism is operative.

### $\Delta H$ and $\Delta S$ Are Varied among Amino Acid Residues.

Before we can propose an assessment of the enthalpy–entropy compensation reported in this study, the individual  $\Delta H$  and  $\Delta S$  values deserve some more specific consideration. The respective  $\Delta H$  and  $\Delta S$  values of those amino acid residues exhibiting near exact compensation behavior are vastly different. For instance, the enthalpic stabilization of pPII for alanine is rather modest but sufficient to outweigh the entropic losses upon conformational ordering to the more compact pPII structure. Surprisingly, the respective enthalpic gain of  $-10$  kJ/mol produced by a  $\beta \rightarrow$  pPII transition in alanine is substantially lower than those of other amino acid residues such as valine ( $-35$  kJ/mol) and isoleucine ( $-70$  kJ/mol), which all have a preference for  $\beta$ . However, as shown in Figure 3, the respective entropies for these residues favor  $\beta$  conformations to such an extent that they overcome (most of

the) enthalpic stabilization of pPII even at room temperature. For valine, the entropic stabilization of  $\beta$ -strand like structures even overcomes enthalpic stabilization conferred in pPII structures at room temperature. The remaining residues all exhibit comparable enthalpic differences between pPII and  $\beta$  with an average enthalpy of approximately  $5$  kJ/mol. The pPII/ $\beta$  equilibria of valine and isoleucine, two aliphatic amino acids with  $C_\beta$  branched side chains, involve particularly large  $\Delta H/\Delta S$  values compared to nonbranched leucine. This result is surprising and will be addressed in further detail below.

### Decomposing the Gibbs Free Energy to Reflect Solvent Mediation.

The near-exact  $\Delta H/\Delta S$  compensation as well as the derived iso-equilibria both point to a common mechanistic effect driving conformational propensities in the unfolded state. The physical origin behind exact thermodynamic compensation is a matter of very multifaceted debates, but it is clear that protein/peptide hydration and solvent reorganization play a key role in conformational changes of peptides and proteins in water.<sup>35–38,40,52,53</sup> For instance, Lumry and Rajender described a two-state hydration model in which the reaction/transition of a protein is coupled to a reaction/transition of water.<sup>35</sup> In this context, the compensation behavior observed here for pPII  $\leftrightarrow$   $\beta$  transitions would be rationalized as a result of direct interaction of hydration shell water with the peptide. Grunwald and Steel proposed a similar theory in which compensation is linked to changes in solvent reorganization, distinguishing between environmental processes in the solvent and nominal reactions of the solute.<sup>37</sup> At the real compensation temperature, the free energy change of the environmental process is zero and hence the  $\Delta G$  associated with the reaction is solely due to the nominal process. To interpret our data we develop a similar concept in that we first assume the total Gibbs energy follows the following balance:

$$\Delta G_\beta = \Delta G_{\beta_c} + \Delta G_{\beta_{ps}} + \Delta G_{\beta_s} \quad (3)$$

where  $\Delta G_{\beta_c}$  is the conformational Gibbs energy difference in vacuo in the absence of intramolecular hydrogen bonding,  $\Delta G_{\beta_{ps}}$  is the peptide solvation Gibbs energy, which encompasses backbone and side chain hydration.  $\Delta G_{\beta_s}$  reflects relaxation processes in the hydration shell which are caused by pPII  $\leftrightarrow$   $\beta$  transitions.

In line with our data, environmental (solvent processes) terms are subject to total enthalpy–entropy compensation at certain compensation temperatures  $T_{C_{ps}}$  and  $T_{C_s}$ . Therefore, we can formulate eq 3 in more explicit terms as

$$\Delta G_\beta = \Delta G_{\beta_c} + \Delta S_{\beta_{ps}}(T_{C_{ps}} - T) + \Delta S_{\beta_s}(T_{C_s} - T) \quad (4)$$

where  $\Delta G_{\beta_{ps}}$  and  $\Delta G_{\beta_s}$  are the entropy differences of peptide–solvent interactions and changes in the configuration of the hydration shell, respectively, which are caused by the increase of the side chains solvent accessible surface upon pPII  $\rightarrow$   $\beta$  conformational transitions.<sup>29</sup> Ben-Naim showed that the purely conformational enthalpies and entropies  $\Delta H_\beta^0$  and  $\Delta S_\beta^0$  do not compensate and that  $\Delta H_{\beta_s} \gg T\Delta S_{\beta_c}$  at room temperature.<sup>53</sup> Following Grunwald and Steel, Ben Naim, and Qian and Hopfield, we assume the Gibbs free energy due to relaxation of the hydration shell is zero (i.e.,  $\Delta G_{\beta_s} = 0$ ,  $T_{C_s} = T$ ) for all temperatures, even though the respective  $\Delta H$  and  $\Delta S$  values can be rather large.<sup>26,27,33</sup> Hence, we can omit the third term and rewrite eq 4 as



$$\Delta G_{\beta} = \Delta H_{\beta_c} + \Delta S_{\beta_{ps}}(T_{C_{ps}} - T) \quad (5)$$

Comparing this equation with the generalized linear equation for entropy–entropy compensation given in eq 2, we can then identify the general compensation temperature  $T_C$  with  $T_{C_{ps}}$  and the constant  $\alpha$  with  $\Delta H_{\beta_c}$ . Thus, our linear fit to  $\Delta H$  vs  $\Delta S$  data (Figure 4) yields an average  $\Delta H_{\beta_c} = -0.770$  kJ/mol, indicating that the change in conformational free enthalpy in the unfolded state favors pPII distributions slightly. The very small value we calculate for  $\alpha$  is diagnostic of what Movileanu and Schiff termed a near-exact compensation.<sup>40</sup> Individual analysis of  $\Delta H/\Delta S$  values for iso-equilibrium cluster 1 (IE1) and 2 (IE2) reveals that IE1 residues (L, V, I, S, K, Y, W, and F) exhibit a lower average conformational enthalpy of  $\Delta H_{\beta_{c,IE1}} = -0.324$  kJ/mol, indicating an even more exact thermodynamic compensation driving propensity among these residues. This low conformational enthalpy is also in line with the rather iso-energetic character of this point ( $\chi_{pPII, IE1}/\chi_{\beta, IE1} \approx 1$ ). On the other hand, cluster 2 residues (E, R, M, N) have a slightly larger conformational enthalpy  $\Delta H_{\beta_{c,IE2}} = -1.49$  kJ/mol. In addition, both clusters exhibit higher compensation temperatures than the average (296.9 K and 302.9 K for clusters 1 and 2, respectively).

Re-examining the series of  $\Delta S_{\beta}$  and  $\Delta H_{\beta}$  values displayed in Figure 2 and listed in Table S2 in the Supporting Information, we observe the largest deviations from the linear compensation fit for alanine ( $\Delta S_{\beta} = -23.0$  J/mol K,  $\Delta H_{\beta} = -10.3$  kJ/mol) and aspartic acid ( $\Delta S_{\beta} = -38.0$  J/mol K,  $\Delta H_{\beta} = -9.2$  kJ/mol). This makes sense as these residues were found to lie outside of the iso-equilibria points (Figure 4c) where  $\Delta G_{\beta_c}$  for the series are approximately equal.

**Rationalizing the Range of  $\Delta H$  and  $\Delta S$  Values: Branched Aliphatics.** Although the above-described model indeed accounts for the obtained enthalpy–entropy compensation, it fails to explain the striking differences among  $\Delta H/\Delta S$  values of (predominantly) aliphatic residues with  $C_{\beta}$  branched (V, I) and linear side chains (K, L, M). The different  $\Delta H$  and  $\Delta S$  values of L and I residues are particularly surprising, since their side chains are very similar, exhibiting comparable surface areas and hydrophobicities, which are both larger than the corresponding values for valine.<sup>29</sup> The same can be said about the so-called conditional hydrophobic accessible surface areas, which Fleming et al. introduced as a crucial determinant for the Gibbs energy of residue conformations.<sup>29</sup> These authors suggested that this surface is generally reduced in pPII compared with  $\beta$  strand conformations hence stabilizing the former via the hydrophobic effect. This, however, would be entropy driven and thus decrease the entropy difference between pPII and the  $\beta$ -strand. Moreover, if the solvent accessible surface area is a measure for this effect, one would expect a hierarchy  $I \approx L > V$ , contrary to our observation. A similar hierarchy would be expected for solvent relaxation processes associated with a change in solvent accessibility. In addition to side-chain solvent interactions one could invoke variations of backbone–solvent interactions due to side chains as the dominant contribution to both  $\Delta H$  and  $\Delta S$  values of pPII/ $\beta$  equilibria, in agreement with Avbelj and Baldwin<sup>25,27</sup> This notion is corroborated by the observed influence of amino acid side chains on the hydration of the N-terminal amide protons in blocked dipeptides, which Bai and Englander determined with hydrogen exchange experiments.<sup>54</sup> The

respective Gibbs energy associated with the HD-exchange shows a  $V \approx I > L$  hierarchy, indicating that V and I are more effective in shielding the peptide from hydration. How this translates into  $\Delta H$  and  $\Delta S$  values remains to be determined, but one could conjecture that the closer proximity of side chain hydrogen atoms to the amide proton in the pPII conformation restricts the torsional degree of freedom of a water molecule hydrogen bonded to the amide proton. This would without doubt reduce the relative entropy of the pPII state further while increasing the corresponding internal energy. Moreover, the highly entropic hydration shell of the side chain could interfere with the hydration sphere of the amide proton.

A complete theory that accounts for how enthalpy–entropy compensation governs amino acid conformation might need an extension beyond the consideration of peptide solvation to account for the differences observed between residues. We wondered whether our results do at least partially reflect different conformational restrictions for branched and linear side chains in pPII and  $\beta$ -strand conformations. To check for this possibility we analyzed the rotamer library of amino acid residues that Dunbrack and Karplus obtained for all amino acid residues from a large set of protein data bank files.<sup>55</sup> On the basis of the positions and widths of distributions reported in our earlier studies,<sup>18,21</sup> we counted the number of side chain rotamers for the following regions of the Ramachandran plot from Figure 2 of Dunbrack and Karplus:  $180^\circ \geq \psi \geq 160^\circ$  and  $-100^\circ \geq \varphi \geq -120^\circ$  for the  $\beta$ -strand of V and I;  $160^\circ \geq \psi \geq 140^\circ$  and  $-100^\circ \geq \varphi \geq -120^\circ$  for the  $\beta$ -strand of K, L, and F;  $180^\circ \geq \psi \geq 160^\circ$  and  $-60^\circ \geq \varphi \geq -100^\circ$  for the pPII-strand of V, I, K, L, and F. Thus, we found that only for V and I the number of rotamers is larger in the  $\beta$ -strand (6 and 4 for V and I) than in the pPII region (3 for V and 0 for I), while the numbers are very similar for K, L, and F (16 and 16, 16 and 15, 6 and 6, respectively). This observation suggests that the rotational degree of freedom of branched side chains is much more restricted in the pPII than in the  $\beta$ -strand region of V and I, whereas no such discrepancy exists for linear side chains. The fact that V and I still share an iso-equilibrium point with four other amino acid residues (including L) suggests a nearly ideal enthalpy–entropy compensation so that steric effects remain absent in the total Gibbs energy balance. Taking this into account, our Gibbs free energy model (eq 5) has to be extended in order to account for enthalpy–entropy compensation brought about by steric restrictions of branched side chains

$$\Delta G_{\beta} = \Delta H_{\beta_c} + \Delta S_{\beta_{ps}}(T_{C_{ps}} - T) + \Delta S_{\beta_{st}}(T_{C_{st}} - T) \quad (6)$$

where  $\Delta S_{\beta_{st}}$  is the new conformational entropy term which is predominantly associated with differences between side chain entropies.

**Implications for Conformational Stability.** These results were interesting and very significant for numerous reasons. First, the coexistence of both compensation effects and iso-equilibria is rare, and indeed this is the first study, which captures and explains this effect for residue level transitions. As discussed above, their occurrence indicates a common source behind promotion of conformational preferences in the unfolded state, which we can directly link to the competing action of peptide solvation. Solvent reorganization might contribute significantly to enthalpy and entropy but does not affect the conformational equilibrium. Second, the coalescence of  $\chi_{pPII}/\chi_{\beta}$  (i.e., the iso-equilibria) suggests that amino acid composition, and hence individual propensities in the unfolded



state, become much less significant near physiological temperatures (310 K). Thus, within the confines of our obtained pPII/ $\beta$  distributions, and in the absence of nearest-neighbor interactions (i.e., solely intrinsic effects), one aspect of the classical random coil model becomes nearly valid at compensation temperatures, namely, the independence of conformational ensembles on the amino acid sequence of peptides and proteins. Therefore, only the different turn-like fractions among the residues matter at these compensation temperatures. Third, the deviation of alanine, aspartic acid, and threonine from iso-equilibrium is very interesting. Aspartic acid and threonine are among a subclass of amino acids which have unusually strong preferences for turn-like conformations which in some cases have been found to be stabilized by side-chain backbone H-bonding.<sup>56,57</sup> How these propensities for turn-like structures affect the thermodynamics of the pPII- $\beta$  equilibrium is unclear. We conjecture that the polar character of the side chains can significantly affect the overall hydration shell of the peptide thus causing a change of the compensation temperature. One might be tempted to consider interactions between the side chains and the terminal groups as well (so-called end effects). However, this can be definitely ruled out for GDG, because Rybka et al. showed that conformational distributions of protonated GDG, AcGDG, and the aspartic acid dipeptide are indistinguishable.<sup>20</sup>

The third amino acid residue that does not share any isoequilibria with other residues is alanine. The conventional explanation, based on several molecular dynamics simulations would invoke a particularly efficient hydration shell packing as the stabilizing factor of pPII.<sup>24</sup> However, in order to invoke protein-hydration as the driving force for pPII stabilization, one would have to assume that the compensation temperature for alanine hydration is much higher for any of the other residues (an estimation puts it way above 400 K, Figure 5c). This is very counterintuitive. A comparison of pPII/ $\beta$  equilibria of trialanine in different mixtures of water with glycerol and ethanol by Toal et al. has recently revealed an enthalpy–entropy compensation with a compensation temperature of 321.5 K. This is perfectly reasonable and would explain some of the enthalpy surplus of pPII for this residue at room temperature but not the observed pPII/ $\beta$  ratio obtained for this peptide (i.e., 8.4). A possible, though unconventional rationale for the high pPII propensity of alanine can be found in the above paper of Toal et al., who report a  $\Delta H_{\beta}^0$  of  $-4.28$  kJ/mol for their enthalpy–entropy plot of cationic AAA.<sup>32</sup> This indicates a rather large stabilization of pPII in vacuo, which is quite surprising in that it contradicts the conventional notion that water is the necessary ingredient for the stabilization of pPII. However, invoking intrinsic forces for the stabilization of pPII is not unprecedented. Raines and co-workers observed that pPII (as opposed to  $\beta$ ) allows for  $n \rightarrow \pi^*$  interactions between  $O_{i-1}(n)$  and  $C_i'=O_i(\pi^*)$  and  $O_{i-1}(n)$  and  $C_i'=N_{i+1}(\pi^*)$  which would stabilize pPII by  $\sim 2.9$  kJ/mol, only slightly lower than the  $\Delta H_{\beta}^0$  value reported by Toal et al.<sup>32</sup> The question arises, however, to what extent these interactions can be modulated by the side chain of a residue.

## CONCLUSION

The results reported in this paper show that the pPII/ $\beta$  equilibrium of amino acids is subject to a nearly exact enthalpy–entropy compensation.<sup>40</sup> We identified two slightly different temperatures at which two subsets of the investigated residues show an isoequilibrium, i.e., they all exhibit the same pPII/ $\beta$  mixture. We attribute the partial compensation to a

combined effect of changes in solvent–solvent, peptide–solvent, and in the case of branched amino acid residues (V and I) to an exact enthalpy–entropy compensation involving conformational restrictions in pPII. Alanine, aspartic acid, and threonine are not part of the two iso-equilibria sets. Alanine is special in that it shows an exceptionally high pPII propensity which might result from a combination of preferential hydration and electronic intrapeptide interactions. Aspartic acid and threonine are known to exhibit an above average propensity for the formation of turn-like conformations stabilized by intrapeptide hydrogen bonding.<sup>20</sup>

What do the reported results tell us about conformational propensities. The picture is complex. If we disregard alanine for a moment, the answer depends on how close the experimental temperature is to the compensation temperature. All pPII propensities increase with  $T_C - T$ . The actual pPII advantage at a given temperature below  $T_C$  depends on the magnitude of  $\Delta H$ . Intrinsic contributions to the propensity can generally be considered as negligible. Alanine, however, might play a different game by exhibiting a much stronger intrinsic contribution to the Gibbs energy that stabilizes pPII.

## ASSOCIATED CONTENT

### Supporting Information

Description of temperature dependence of valine's  $^3J$  coupling constant; table of conformationally sensitive  $\Delta\epsilon_{\text{pPII}}$  and  $\Delta\epsilon_{\beta}$  parameters; table of  $\Delta H$  and  $\Delta S$  values between pPII and  $\beta$ ; discussion of enthalpy–entropy compensation for amino acid residues exhibiting isoequilibrium behavior; description of error analysis; table of thermodynamic errors; and references. This material is available free of charge via the Internet at <http://pubs.acs.org>.

## AUTHOR INFORMATION

### Corresponding Author

\*Phone: 215-895-2268. Fax: 215-895-1265. E-mail: [rschweitzer-stenner@drexel.edu](mailto:rschweitzer-stenner@drexel.edu).

### Present Address

<sup>§</sup>D.J.V.: School of Medicine, Washington University, St. Louis, MO 63110.

### Notes

The authors declare no competing financial interest.

## ACKNOWLEDGMENTS

We like to acknowledge earlier measurements of  $^1\text{H}$  NMR spectra of GxG peptides by Mr. Hendrik Elsner, at that time a high school student from Germany. The work was supported in part by a grant from the National Science Foundation (Grant Chem 0939972) and by research fellowships from the College of Arts and Sciences of Drexel University.

## REFERENCES

- (1) Uversky, V. N.; Oldfield, C. J.; Dunker, K. A. Showing Your Id: Intrinsic Disorder as an Id for Recognition, Regulation and Cell Signalling. *J. Mol. Recognit.* **2005**, *18*, 343–384.
- (2) Uversky, V.; Dunker, A. K. Why Are We Interested in the Unfolded Peptides and Proteins? In *Protein and Peptide Folding, Misfolding, and Non-Folding*; Schweitzer-Stenner, R., Ed.; Wiley & Sons: Hoboken, NJ, 2012; pp 3–54.
- (3) Dunker, A. K.; Cortese, M. S.; Romero, P.; Iakoucheva, I. M.; Uversky, V. N. Flexible Nets. The Roles of Intrinsic Disorder in Protein Interaction Networks. *FEBS J.* **2005**, *272*, 5129–5148.

- (4) Mohan, A.; Oldfield, C. J.; Radivojac, P.; Vacic, V.; Cortese, M. S.; Dunker, A. K.; Uversky, V. N. Analysis of Molecular Recognition Features (Morfs). *J. Mol. Biol.* **2006**, *362*, 1043–1059.
- (5) Oldfield, C. J.; Meng, J.; Yang, J. Y.; Yang, M. Q.; Uversky, V. N.; Dunker, A. K. Flexible Nets: Disorder and Induced Fit in the Association of P53 and 14–3-3 with Their Partners. *BMC Genomics* **2008**, *9*, 1–20.
- (6) Brant, D. A.; Flory, P. J. J. The Configuration of Random Polypeptide Chains. II. Theory. *J. Am. Chem. Soc.* **1965**, *87*, 2791–2800.
- (7) Flory, P. J. *Statistical Mechanics of Chain Molecules*; Wiley & Sons: New York, 1969; pp 30–31.
- (8) Tanford, C. Protein Denaturation. *Adv. Protein Chem.* **1968**, *23*, 121–282.
- (9) Ramachandran, G. N.; Ramachandran, C.; Sasisekharan, V. Stereochemistry of Polypeptide Chain Configurations. *J. Mol. Biol.* **1963**, *7*, 95–99.
- (10) Pappu, R. V.; Rose, G. D. A Simple Model for Polyproline II Structure in Unfolded States of Alanine-Based Peptides. *Protein Sci.* **2002**, *11*, 2437–2455.
- (11) Pappu, R. V.; Srinivasan, R.; Rose, G. D. The Flory Isolated-Pair Hypothesis Is Not Valid for Polypeptide Chains: Implications for Protein Folding. *Proc. Natl. Acad. Sci. U.S.A.* **2000**, *97*, 12565–12570.
- (12) Dyson, H. J.; Wright, P. E. Insights into the Structure and Dynamics of Unfolded Proteins from Nuclear Magnetic Resonance. *Adv. Protein Chem.* **2002**, *62*, 311–340.
- (13) Dyson, H. J.; Wright, P. E. Unfolded Proteins and Protein Folding Studied by Nmr. *Chem. Rev.* **2004**, *104*, 3607–3622.
- (14) Bernado, P.; Blanchard, L.; Timminis, P.; Marion, D.; Rugrok, R. W. H.; Blackledge, M. A Structural Model for Unfolded Proteins from Dipolar Couplings and Small-Angle X-Ray Scattering. *Proc. Natl. Acad. Sci. U.S.A.* **2005**, *102*, 17002–17007.
- (15) Bernado, P.; Mylonas, E.; Petoukhov, M. V.; Blackledge, M.; Svergun, D. I. Structural Characterization of Flexible Proteins Using Small-Angle X-Ray Scattering. *J. Am. Chem. Soc.* **2007**, *129*, 5656–5664.
- (16) Bernado, P.; Bertoncini, C. W.; Griesinger, C.; Zweckstetter, M.; Blackledge, M. Defining Long-Range Order and Local Disorder in Native  $\alpha$ -Synuclein Using Residual Dipolar Couplings. *J. Am. Chem. Soc.* **2005**, *127*, 17968–17969.
- (17) Sziegat, F.; Silvers, R.; Hähnke, M. J.; Jensen, M. R.; Blackledge, M.; Wirmer-Bartschek, J.; Schwalbe, H. Disentangling the Coil: Modulation of Conformational and Dynamic Properties by Site-Directed Mutation in the Non-Native State of Hen Egg White Lysozyme. *Biochemistry* **2012**, *51*, 3361–3372.
- (18) Hagarman, A.; Measey, T. J.; Mathieu, D.; Schwalbe, H.; Schweitzer-Stenner, R. Intrinsic Propensities of Amino Acid Residues in Gxg Peptides Inferred from Amide I Band Profiles and Nmr Scalar Coupling Constants. *J. Am. Chem. Soc.* **2010**, *132*, 540–551.
- (19) Hagarman, A.; Mathieu, D.; Toal, S.; Measey, T. J.; Schwalbe, H.; Schweitzer-Stenner, R. Amino Acids with Hydrogen-Bonding Side Chains Have an Intrinsic Propensity to Sample Various Turn Conformations in Aqueous Solution. *Chem.—Eur. J.* **2011**, *17*, 6789–6797.
- (20) Rybka, K.; Toal, S. E.; Verbaro, D. J.; Mathieu, D.; Schwalbe, H.; Schweitzer-Stenner, R. Disorder and Order in Unfolded and Disordered Peptides and Proteins: A View Derived from Tripeptide Conformational Analysis. I. Tripeptides with Long and Predominantly Hydrophobic Side Chains. *Proteins* **2013**, *81*, 955–967.
- (21) Schweitzer-Stenner, R.; Hagarman, A.; Toal, S.; Mathieu, D.; Schwalbe, H. Disorder and Order in Unfolded and Disordered Peptides and Proteins: A View Derived from Tripeptide Conformational Analysis. II. Tripeptides with Short Side Chains Populating  $\alpha$ -x and  $\beta$ -Type Like Turn Conformations. *Proteins* **2013**, *81*, 968–983.
- (22) Toal, S.; Meral, D.; Verbaro, D.; Urbanc, B.; Schweitzer-Stenner, R. pH-Independence of Trialanine and the Effects of Termini Blocking in Short Peptides: A Combined Vibrational, NMR, UVCD, and Molecular Dynamics Study. *J. Phys. Chem. B* **2013**, *117*, 3689–3706.
- (23) Han, W.-G.; Jakanen, K. J.; Elstner, M.; Suhai, S. Theoretical Study of Aqueous N-Acetyl-L-Alanine N-Methylamide: Structures and Raman, VCD, and ROA Spectra. *J. Phys. Chem. B* **1998**, *102*, 2587–2602.
- (24) Garcia, A. E. Characterization of Non-Alpha Conformations in Ala Peptides. *Polymer* **2004**, *120*, 885–890.
- (25) Avbelj, F.; Gradolnik, S. G.; Gradolnik, J.; Baldwin, R. L. Intrinsic Backbone Preferences Are Fully Present in Blocked Amino Acids. *Proc. Natl. Acad. Sci. U.S.A.* **2006**, *103*, 1272–1277.
- (26) Tran, H. T.; Wang, X.; Pappu, R. V. Reconciling Observations of Sequence-Specific Conformational Properties with Generic Polymeric Behavior of Denatured Proteins. *Biochemistry* **2005**, *44*, 11369–11380.
- (27) Avbelj, F. Solvation and Electrostatics as Determined of Local Structural Order in Unfolded Peptides and Proteins. In *Protein and Peptide Folding, Misfolding and Non-Folding*; Schweitzer-Stenner, R., Ed. John Wiley & Sons: Hoboken, NJ, 2012; pp 131–158.
- (28) Avbelj, F.; Baldwin, R. L. Role of Backbone Solvation and Electrostatics in Generating Preferred Peptide Backbone Conformations: Distributions of  $\Phi$ . *Proc. Natl. Acad. Sci. U.S.A.* **2003**, *100*, 5742–5747.
- (29) Fleming, P. J.; Fitzkee, N. C.; Mezei, M.; Srinivasan, R.; Rose, G. D. A Novel Method Reveals That Solvent Water Favors Polyproline II over B-Strand Conformation on Peptides and Unfolded Proteins: Conditional Hydrophobic Accessible Surface Areas (Chasa). *Protein Sci.* **2005**, *14*, 111–118.
- (30) Shi, Z.; Chen, K.; Liu, Z.; Ng, A.; Bracken, W. C.; Kallenbach, N. R. Polyproline II Propensities from Gxgg Peptides Reveal an Anticorrelation with B-Sheet Scales. *Proc. Natl. Acad. Sci. U.S.A.* **2005**, *102*, 17964–17968.
- (31) Eker, F.; Griebenow, K.; Schweitzer-Stenner, R. Stable Conformations of Tripeptides in Aqueous Solution Studied by UV Circular Dichroism Spectroscopy. *J. Am. Chem. Soc.* **2003**, *125*, 8178–8185.
- (32) Toal, S.; Omid, A.; Schweitzer-Stenner, R. Conformational Changes of Trialanine Induced by Direct Interactions between Alanine Residues and Alcohols in Binary Mixtures of Water with Glycerol and Ethanol. *J. Am. Chem. Soc.* **2011**, *133*, 12728.
- (33) Shi, Z.; Woody, R. W.; Kallenbach, N. R. Is Polyproline II a Major Backbone Conformation in Unfolded Proteins? *Adv. Protein Chem.* **2002**, *62*, 163–240.
- (34) Yang, W. Y.; Larios, E.; Gruebele, M. On the Extended B-Conformation of Polypeptides at High Temperatures. *J. Am. Chem. Soc.* **2003**, *125*, 16220–16227.
- (35) Lumry, R.; Shyamala, R. Enthalpy-Entropy Compensation Phenomena in Water Solutions of Proteins and Small Molecules: A Ubiquitous Property of Water. *Biopolymers* **1970**, *9*, 1125–1227.
- (36) Dunitz, J. D. Win Some, Lose Some: Enthalpy-Entropy Compensation in Weak Intermolecular Interactions. *Chem. Biol.* **1995**, *2*, 709–712.
- (37) Grunwald, E.; Steel, C. Solvent Reorganization and Thermodynamic Enthalpy-Entropy Compensation. *J. Am. Chem. Soc.* **1995**, *117*, 5687–5692.
- (38) Liu, L.; Guo, Q.-X. Isokinetic Relationship, Isoequilibrium Relationship and Enthalpy-Entropy Compensation. *Chem. Rev.* **2001**, *101*, 673–695.
- (39) Schweitzer-Stenner, R.; Measey, T.; Hagarman, A.; Dragomir, I. The Structure of Unfolded Peptides and Proteins Explored by Raman and IR Spectroscopies. In *Vibrational Spectroscopy on Peptides and Proteins*; Longhi, S.; Uversky, V. N., Eds.; Wiley & Sons: Chichester, U.K., 2010; p 117–224.
- (40) Movileanu, L.; Schiff, E. A. Entropy-Enthalpy Compensation of Biomolecular Systems in Aqueous Phase: A Dry Perspective. *Montash Chem.* **2013**, *144*, 59–56.
- (41) Oh, K.-I.; Jung, Y.-S.; Hwang, G.-S.; Cho, M. Conformational Distributions of Denatured and Unstructured Proteins Are Similar to Those of 20  $\times$  20 Blocked Dipeptides. *J. Biomol. NMR* **2012**, *53*, 25–41.
- (42) Oh, K.-I.; Lee, K.-K.; Park, E.-K.; Jung, Y.-S.; Hwang, G.-S.; Cho, M. A Comprehensive Library of Blocked Dipeptides Reveals Intrinsic

Backbone Conformational Propensities of Unfolded Proteins. *Proteins Struct. Funct. Genet.* **2012**, *80*, 977–990.

(43) Oh, K.-I.; Lee, K.-K.; Park, E. K.; Kwang, G. S.; Cho, M. Circular Dichroism Eigenspectra of Polyproline II and B-Strand Conformers of Trialanine in Water: Singular Value Decomposition Analysis. *Chirality* **2010**, *22*, E186–E201.

(44) Kelly, M. A.; Chellgren, B. W.; Rucker, A. L.; Troutman, J. M.; Fried, M. G.; Miller, A.; Creamer, T. P. Host-Guest Study of Left Handed Polyproline II Helix Formation. *Biochemistry* **2001**, *2001*, 14376–14383.

(45) Tiffany, M. L.; Krimm, S. New Chain Conformations of Poly(Glutamicacid) and Polylysine. *Biopolymers* **1968**, *6*, 1767–1770.

(46) Woody, R. W. Circular Dichroism Spectrum of Peptides in the Poly(Pro)II Conformation. *J. Am. Chem. Soc.* **2009**, *131*, 8234–8245.

(47) Shi, Z.; Olson, C. A.; Rose, G. D.; Baldwin, R. L.; Kallenbach, N. R. Polyproline II Structure in a Sequence of Seven Alanine Residues. *Proc. Natl. Acad. Sci. U.S.A.* **2002**, *99*, 9190–9195.

(48) Karplus, M. Theoretical Calculation Links NMR Coupling Constant to Molecular Geometry. *J. Chem. Phys.* **1959**, *30*, 11–15.

(49) Wang, A. C.; Bax, A. Determination of the Backbone Dihedral Angles Phi in Human Ubiquitin from Reparametrized Empirical Karplus Equations. *J. Am. Chem. Soc.* **1996**, *118*, 2483–2494.

(50) Beasley, J. R.; Doyle, D. F.; Cohen, D. S.; Fine, B. R.; Pielak, G. J. Searching for Quantitative Entropy-Enthalpy Compensation among Protein Variants. *Proteins* **2002**, *49*, 398–402.

(51) Krug, R. R.; Hunter, W. G.; Grieger, R. A. Enthalpy-Entropy Compensation. I. Some Fundamental Statistical Problems Associated with the Analysis of Van't Hoff and Arrhenius Data. *J. Phys. Chem.* **1976**, *80*, 2335–2341.

(52) Qian, H.; Hopfield, J. J. Entropy-Enthalpy Compensation: Perturbation and Relaxation in Thermodynamic Systems. *J. Chem. Phys.* **1996**, *105*, 9292–9298.

(53) Ben Naim, A., *Molecular Theory of Water and Aqueous Solutions-Part I: Understanding Water*; World Scientific: Singapore, 2009.

(54) Bai, Y.; Milne, J. S.; Mayne, L.; Englander, S. W. Primary Structure Effects on Peptide Group Hydrogen Exchange. *Proteins* **1993**, *17*, 75–86.

(55) Dunbrack, R. L.; Karplus, M. Backbone-Dependent Rotamer Library for Proteins. Application to Side Chain Prediction. *J. Mol. Biol.* **1993**, *230*, 543–574.

(56) Verbaro, D.; Mathieu, D.; Toal, S. E.; Schwalbe, H.; Schweitzer-Stenner, R. Inoized Trilysine: A Model System for Understanding the Nonrandom Structure of Poly-L-Lysine and Lysine-Containing Motifs in Proteins. *J. Phys. Chem. B* **2012**, *116*, 8084–8094.

(57) Duitch, L.; Toal, S.; Measey, T. J.; Schweitzer-Stenner, R. Triaspartate: A Model System for Conformationally Flexible DDD Motifs in Proteins. *J. Phys. Chem. B* **2012**, *116*, 5160–5171.